

University of Vermont

UVM ScholarWorks

Graduate College Dissertations and Theses

Dissertations and Theses

2023

Developing Muscle Synergy Functions For Remote Gait Analysis

Nicole Marie Donahue

University of Vermont

Follow this and additional works at: <https://scholarworks.uvm.edu/graddis>



Part of the [Computer Sciences Commons](#)

Recommended Citation

Donahue, Nicole Marie, "Developing Muscle Synergy Functions For Remote Gait Analysis" (2023).

Graduate College Dissertations and Theses. 1656.

<https://scholarworks.uvm.edu/graddis/1656>

This Thesis is brought to you for free and open access by the Dissertations and Theses at UVM ScholarWorks. It has been accepted for inclusion in Graduate College Dissertations and Theses by an authorized administrator of UVM ScholarWorks. For more information, please contact schwirks@uvm.edu.

DEVELOPING MUSCLE SYNERGY FUNCTIONS FOR REMOTE GAIT ANALYSIS

A Thesis Presented

by

Nicole Donahue

to

The Faculty of the Graduate College

of

The University of Vermont

In Partial Fulfillment of the Requirements
for the Degree of Master of Science
Specializing in Biomedical Engineering

May, 2023

Defense Date: December 12, 2022
Thesis Examination Committee:

Ryan S. McGinnis, Ph.D., Advisor
Nick Cheney, Ph.D., Chairperson
Niccolo Fiorentino, Ph.D.
Reed Gurchiek, Ph.D.
Cynthia J. Forehand, Ph.D., Dean of the Graduate College

ABSTRACT

Digital medicine promises to improve healthcare and enable its delivery to rural and underserved communities. A key component of digital medicine is accurate and robust remote patient monitoring. For example, remote monitoring of biomechanical measures of limb impairment during daily life could allow near real-time tracking of rehabilitation progress and personalization of rehabilitation paradigms in those recovering from orthopedic surgery. Wearable sensors have long been suggested as a means for quantifying muscle and joint loading, which can provide a direct measure of limb impairment. However, current approaches either do not provide these measures or require unwieldy wearable sensor arrays and/or in-person calibration activities that limit their use. In this thesis, I advance the use of muscle synergy functions, which leverage the synergistic relationship within a group of muscles, to reduce the complexity of wearable sensor arrays and overcome the current need for an in-person visit to a human performance laboratory for calibration. Surface electromyography (EMG) and kinematic data were recorded from leg muscles and segments of nine healthy subjects during walking. Subject-general muscle synergy models were validated using the leave-one-subject-out method for 4 different pairs of input muscle model sets using filtered EMG data. The effect of adding kinematic data (angular velocity) from thigh and shank segment locations was investigated. The average correlation between true and estimated excitations was 96% higher when angular velocity data was included in the 4-muscle input model set. The estimated excitations informed muscle activations with 6.7% mean absolute error (MAE) and 43% variance accounted for (VAF) averaged across all muscles when kinematic data was included in the model, and 7.3% MAE and 43% VAF without kinematic data. These results lay the groundwork for developing muscle synergy functions that no longer require in-person calibration, paving the way for completely remote studies of muscle and joint loading.

ACKNOWLEDGEMENTS

I would like to thank my advisor Dr. Ryan McGinnis for his encouragement and mentorship towards my becoming a biomedical engineer and his counsel during my journey to completing a master's degree. When I started working with him in 2018, I knew I found my place here and realized biomedical engineering was my future. Dr. McGinnis included me as a valued member of his team immediately and he has been my anchor these past four years.

Next, I would like to thank Dr. Reed Gurchiek for his guidance, mentorship, and infectious enthusiasm during our discussions on biomechanics and neuromusculoskeletal modeling. Dr. Gurchiek's work is my foundation. He generously shared his insights of biomedical engineering and research, and whether he was on campus here at UVM or Stanford, I could always count on him to help me.

Next, I would like to thank Dr. Niccolo Fiorentino for always making me feel like an integral member of the teaching team as a teaching assistant and for giving me the opportunity to teach what I learned and share my enthusiasm for biomedical engineering with the students.

And finally, my thanks to Dr. Nick Cheney who so willingly and graciously said yes to being my chairperson. I appreciate his ability to step into the role to support my achieving

a master's degree, and the wisdom for knowing what needed to be done to get to the finish line.

I would like to thank my teammates in the M-Sense Research Group for their continuous support and making every day we spent in the lab together fun. A special thanks to my mentees Shannon, Ian, and Justine for all of their contributions to the Joint and Muscle Monitoring System and motion capture data processing!

To my family and friends, I love you all so much! I could not have done this without you. Even though Massachusetts is a three hour drive to Burlington, you were only a phone call away. I am truly grateful for my strong network of support. Thank you all for having my back during the peaks and valleys of my journey.

TABLE OF CONTENTS

	Page
ACKNOWLEDGEMENTS.....	ii
LIST OF TABLES.....	vii
LIST OF FIGURES.....	viii
CHAPTER 1: INTRODUCTION.....	1
1.1. Wearable Sensors for Remote Gait Analysis.....	1
1.2. Motivation to Study Movement.....	4
1.3. Executive Overview.....	5
CHAPTER 2: BIOMECHANICS AND MUSCLE FUNCTION.....	7
2.1. Muscle Function and Activity.....	7
2.2. Gait Adaptations.....	8
2.3. Muscle Synergies.....	8
2.4. Neuromusculoskeletal Modeling.....	10
CHAPTER 3: PRIOR WORK.....	12
3.1. Prior Work: Subject-Specific Muscle Synergy Model.....	12
3.2. Gap Analysis.....	14
3.3. Defined Aims.....	15

CHAPTER 4: DATA METHODS.....	17
4.1. Participants and Data Collection.....	17
4.2. Signal Processing Techniques.....	19
4.2.1. Electromyography Signal.....	19
4.2.2. Gyroscope Signals.....	20
CHAPTER 5: SUBJECT-GENERAL MUSCLE SYNERGY MODELS.....	22
5.1. Problem Statement.....	22
5.2. Methods.....	23
5.3. Results.....	24
5.4. Discussion.....	28
CHAPTER 6: EFFECT OF KINEMATIC DATA.....	31
6.1. Problem Statement.....	31
6.2. Methods.....	33
6.3. Results.....	35
6.4. Discussion.....	40
CHAPTER 7: FUTURE WORK.....	42
7.1. Future Work.....	42
7.2. Joint and Muscle Monitoring System (JAMMS).....	43
7.2.1. Motivation.....	43
7.2.2. Project Overview.....	44
7.2.3. Evolution of JAMMS.....	45

CHAPTER 8: CONCLUDING REMARKS.....	47
8.1. Conclusion.....	47
REFERENCES.....	48
APPENDIX.....	55

LIST OF TABLES

Table	Page
Table 1: Summary statistics for MG muscle for 4-, 3-, 2-, and 1- muscle input Subject general models and the results of the subject-specific model in parentheses to compare, apart from the single muscle model.....	27
Table 2: Comparison of different parameter settings for 5-subject, 4-muscle input model after the addition of kinematic data.....	36
Table 3: Comparison of different parameter settings for 9-subject, 4-muscle input model after the addition of kinematic data.....	37
Table 4: Comparison of the summary statistics between the kinematic (kin.), i.e. Trial 7 and no kinematic (no kin.) 9-subject, 4-muscle input subject general model.....	39

LIST OF FIGURES

Figure	Page
Figure 1: Knee flexor (left) and extensor (right) synergistic muscle groups responsible for flexion and extension of the knee during walking.....	9
Figure 2: Overview of the forward dynamics approach to neuromusculoskeletal modeling to estimate muscle forces and joint moments given the neural signal (EMG) [50].....	11
Figure 3: Example of a NMS model of the lower extremities created in Open-Sim [52].....	11
Figure 4: Visual overview of muscle excitation estimation procedure from [30] where there are four measured excitations input into the synergy functions to estimate the six unmeasured output excitations.....	13
Figure 5: Anatomical diagram of EMG and IMU sensor placement locations on cartoon leg on the front (left) and back (right) view of the right leg. IMU sensors are illustrated in light grey and EMG sensors are illustrated in dark grey with corresponding labels of the sensor location names.....	18
Figure 6: Electromyography signal from a subject's medial gastrocnemius during walking, before filtering.....	19
Figure 7: Electromyography signal from a subject's medial gastrocnemius during walking, after filtering.....	20
Figure 8: Gyroscope signal from a subject's lower leg (shank) segment during walking, before filtering.....	21
Figure 9: Gyroscope signal from a subject's lower leg (shank) segment during walking, after filtering.....	21
Figure 10: Visual overview of how the subject-general model works.....	23
Figure 11: Results of the true vs. estimate signal of the MG muscle for the 4-muscle input model for Subject 1.....	26

Figure 12: Visual summary of the statistical results for the 4-muscle input model across all subjects for each muscle excitation that was estimated and how they compare to the subject-specific results (RMSE and MAE values are expressed in units percentage of MVC).....	27
Figure 13: Conceptual plot of the lower limb segment angular velocity during stance and swing phase [60]	32
Figure 14: Angular velocity of the shank segment during three walking strides With the peak angular velocity between two blue lines which highlight swing phase.....	32
Figure 15: Visual summary of the performance of the 4-muscle input model with varying parameters (number of iterations, observations and subjects) to describe how the affect performance (average correlation across all of the estimated muscles, expressed as a percentage).....	38
Figure 16: Latest prototype of JAMMS, a custom knee sleeve instrumented with two EMG and two IMU sensors, a PCB and battery. The IMU sensors and PCB are contained in 3D-printed casing.....	46

CHAPTER 1: INTRODUCTION

1.1. Wearable Sensors for Remote Gait Analysis

The remote health monitoring revolution is driven by the ability to collect data in robust ways. Wearable sensors have long been suggested as a means for measuring human movement [1,2]. Consumer demand for lightweight, wearable devices such as smartwatches has reduced the cost and bulkiness of sensing and computational technology. This has greatly increased the broad span of possibilities for acquiring human movement data from many different populations (e.g. [3-6]). The applications of wearable sensors for remote gait analysis are exciting and innovative. Wearable sensors have the ability to collect data about patients' muscle function and activity levels during walking without a visit to their clinician's office nor self-reporting, as self-reported levels of activity often differ from actual levels of activity [7].

The use of surface electromyography (sEMG, EMG) signals is an emerging technique in gait analysis and wearable sensor based remote patient monitoring to measure the excitations of muscles [8]. sEMG has been used for decades to evaluate neuromuscular responses during a range of activities and develop rehabilitation protocols. Surface electromyography combined with kinematic and kinetic data is a useful tool for decision making of the appropriate methods needed to treat patients and is an important parameter for a dynamic assessment of muscle strength in gait analysis [9].

For example, Multiple Sclerosis is a chronic neurodegenerative disease. People with Multiple Sclerosis (PwMS) often experience ankle joint contractures which results in the inability to dorsiflex their feet. This can lead to a decline in performance of daily balance

challenge activities like gait and increases their risk of falls (e.g., [3,10-14]). Gait impairments are commonly assessed using functional tests such as the timed-up-and-go, but these tests lack the sensitivity to detect changes in gait quality [15]. Using sEMG to measure muscle activity of dorsiflexor muscles such as the tibialis anterior can reveal increased or delayed peaks in muscle activation patterns and be used to inform rehabilitation [16].

Additionally, fear of reinjury is an important factor in determining who returns to sport following an anterior cruciate ligament reconstruction (ACLR). Fear of reinjury is a psychological response to injury that can negatively affect rehabilitation outcomes, including preventing a successful return to sport [17]. Athletes with fear of reinjury may reduce their participation in physical activities where they can potentially reinjure themselves. Due to the extended time of inactivity, cautious feelings and muscular atrophy caused by the injury, this often results in stiffened movement patterns and lowered strength and range of motion when returning to dynamic tasks. The combination of pain, reduced activity and muscle weakness is also directly associated with compensation patterns and favorable adaptations. EMG can be used to measure muscle activity in the quadriceps muscles to look for signs of weakened performance and monitor muscle and joint loading. Tracking muscle weakness alone via EMG can give insight into loading patterns and restore athlete's confidence in their muscle function (e.g., [4,18,19]). Then, evaluations can be done to determine if athletes should be evaluated for psychological and emotional consequences of injury in addition to the physical compensations as they appear to be related [20]. Lastly, crouch gait is characterized as reduced strength which causes excessive

ankle dorsiflexion, knee and hip flexion and is common in patients with cerebral palsy (CP). As it worsens over time, sEMG can be used to measure muscle activity in the lower extremities and track progression of these symptoms [21].

EMG can be measured with low profile wearable sensors like Biostamps (Biostamp, MC10, Lexington, MA, USA) that adhere to the skin and do not require any additional wiring. There are many advantages of understanding muscle activation patterns in both healthy and impaired populations. However, traditional EMG approaches require instrumenting many muscles. This process often requires patients to come into a human performance laboratory, which isn't always feasible. Other challenges include limited access to these laboratories, as there are relatively few in the U.S., and the cost of assessments in a performance lab.

The most widely used wearable sensors are inertial measurement units (accelerometer and gyroscope packaged together). Inertial measurement units (IMUs) are small and lightweight, which make them a convenient and practical choice for mobile measurements outside the laboratory. Recent advancements have further facilitated new opportunities to utilize this technology for remote gait analysis [22]. Simple systems involving a single accelerometer have been used to detect various temporal parameters such as stride length, step count, cadence, and walking speed [23-27]. More complex systems have been created with arrays of electromyography sensors, accelerometers, gyroscopes, and goniometers to measure segment and joint kinematics and estimate muscle forces amongst other uses (e.g., [4,18,28-32])

1.2. Motivation to Study Movement

Walking is a basic human movement. For the general population, in order to get from one location to the next, there is going to be walking involved. Studying walking helps to understand Central Nervous System (CNS) communication, i.e. how the brain controls and coordinates these movements by sending neural signals to the body. When these neural pathways are disrupted, results can manifest in ways that negatively impact someone's ability to control their own body. This information can be used to advance research in the biomedical field and current remote health monitoring techniques.

It is important to study how people walk because gait adaptations can give us insight into the physiological, neural and psychological adaptations someone makes to adapt to their environment in both healthy and impaired populations [3,14]. This is done by observing spatio-temporal gait parameters such as muscle activation timing, walking speed, cadence, step duration and stride length [23-25]. All measurements which can be taken inside a motion capture lab when a person is outfitted with wearable sensors and reflective markers. Studying these parameters reveals patterns among populations with certain neuromusculoskeletal disorders such as Multiple Sclerosis (MS) or Parkinson's Disease [33,34]. Four common clinical applications of wearable sensors are identifying movement disorders, assessing surgical outcomes, identifying reduced loading and walking instability [22].

There is increasing potential for wearable sensors for remote gait assessment to enable interventions during the post-operative recovery period. Remote monitoring of biomechanical measures of limb impairment during daily life could allow near real-time

tracking of rehabilitation progress and personalization of rehabilitation paradigms in those recovering from orthopedic surgery.

There is an increasing need for coordination of care via remote health in rural and underserved communities. Rural Vermont residents' health is challenged by healthcare costs, chronic disease management and policy decisions differentially funding for health services in rural communities [35,36]. Wearable sensors and other digital medicine technology may be especially beneficial in providing rural health clinics with the technology to remotely monitor the health and environmental exposures of their patients. The deployment of such technologies require accurate and robust solutions.

1.3. Executive Overview

Wearable sensors have long been suggested as a means for quantifying muscle and joint loading, which can provide a direct measure of limb impairment. However, current approaches either do not provide these measures or require unwieldy wearable sensor arrays and/or in-person calibration activities that limit their use [37]. The remaining sections of the thesis illustrate the background information (Chapter 2), prior work (Chapter 3) and data collection methods (Chapter 4).

In this thesis, I advance the use of muscle synergy functions [38-40], which leverage the synergistic relationship within a group of muscles, to reduce the complexity of wearable sensor arrays and overcome the current need for an in-person visit to a human performance laboratory for calibration. The goal of this work is to reduce the number of wearable sensors required for remote monitoring of joint and muscle loading. In the first Aim, subject-general muscle synergy models were validated using the leave-one-subject-out method for

4 different pairs of input muscle model sets using filtered EMG data. In the second Aim, the effect of adding kinematic data (angular velocity) from thigh and shank segment locations was investigated. The focus of Chapters 5 and 6 are the results and discussions of Aims 1 and 2 respectively. Lastly, Chapter 7 includes the concluding remarks and next steps for this work and discusses the project in which this work is to be deployed for commercialization. This work lays the groundwork for developing muscle synergy functions that no longer require in-person calibration, paving the way for completely remote studies of muscle and joint loading.

CHAPTER 2: BIOMECHANICS AND MUSCLE FUNCTION

2.1. Muscle Function and Activity

Muscle function is defined as one's ability to be able to contract their muscles at the time they intend to, to perform the movements they intend to. Muscle activity (or activation of muscles) is the contraction. It is measured by how much force one can exert. Clinicians and physical therapists use muscle function and activity to understand how joints and muscles are loaded during activities of daily living, especially while recovering from an injury or surgery such as an anterior-cruciate ligament (ACL) repair [4,18,29,41,42]. When the body performs a motor task, the CNS excites muscles to develop forces that are transmitted by tendons to the skeleton to direct the action. Muscle excitations alone provide clinical insight to motor control [2]. For example, muscle activation patterns are a result of the timing of different neurons firing to activate groups of muscles when completing a specific movement. Following pain or injury, neuromuscular inhibition of these neurons may develop. This results in changes to the control and function of the affected area [43]. The long-term effect of this can have a negative impact on a patient's quality of life.

Studying muscle function also helps to understand muscle growth and strengthening of muscles during exercise and rehabilitation [44]. Depending on the technology they have available, athletes and personal trainers use muscle strength tests as a way to gauge strength or endurance and identify gaps in training to inform training plans [42,45].

2.2. Gait Adaptations

Gait adaptations describe how a person's gait changes as people adapt to their physical limitations. Conditions such as aging, injury or neurodegenerative disorders reduce the capacity for generating muscle force. In turn, people compensate to accommodate their limitations to their lifestyle. Changes in gait such as reduced walking speed and step length and increased double support time are well documented in literature and by clinical observation but not well understood [10,27,46-48]. Gait adaptations can give insight into the physiological, neural and psychological adaptations someone makes to adapt to their physical capacity in both healthy and impaired populations because adaptations that can be measured may be markers of disease. Recent studies suggest that different NMS adaptations underlie the resulting kinematic and kinetic patterns of the lower extremities during gait. Impairments such as knee pain, stiffness, and quadriceps weakness as a result of knee osteoarthritis influence compensatory actions which cause functional limitations. Wearable sensors can track such kinematic changes in patients while they go about their daily life.

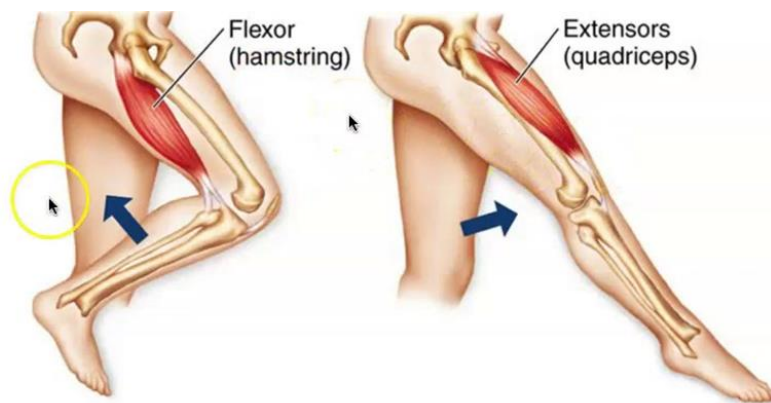
2.3. Muscle Synergies

The CNS recruits muscles to work together to generate the complex movements of the human body. To reduce the complexity of this recruitment process, synergistic muscle groups are often recruited together. Muscle synergies refer to a low-dimensional representation of multiple EMG time-series of this phenomena. A single muscle can be part of multiple synergistic muscle groups, and a single group can activate various muscles.

Muscle synergies describe the activation of a subset of muscles that contribute to a particular movement, thus reducing the dimensionality of muscle control. Muscle synergy functions describe the synergistic relationship between a subset of muscles [38]. Muscles in different synergistic groups work together at specific activation timing to be able to coordinate the movement observed when someone walks. For example, Figure 1 is the knee flexor and extensor synergistic muscle groups. They are the groups of muscles responsible for flexion and extension of the knee during walking. Studying muscle synergies can give insight to how the muscles are recruited by the CNS since this recruitment process is not well understood [49]. We can also learn how this recruitment might change when someone has a neurodegenerative disease like MS, or if someone is going through gait retraining after, for example, a knee replacement.

Figure 1:

Knee flexor (left) and extensor (right) synergistic muscle groups responsible for flexion and extension of the knee during walking.



2.4. Neuromusculoskeletal Modeling

One aim of neuromusculoskeletal models is to estimate or predict muscle forces, joint moments, and/or joint kinetics from neural signals (EMG). Muscle activation dynamics govern the transformation from the neural signal to a measure of muscle activation. Muscle contraction dynamics characterize how the muscle activations are transformed into muscle forces. Given a model of the musculoskeletal geometry, joint moments can be estimated from aforementioned forces. Lastly, the equations of motion allow joint moments to be transformed into joint movements [50]. This process is described in Figure 2. Figure 3 is an example of a model depicting the musculoskeletal geometry of the lower extremities. When data is collected using motion capture technology in a human performance laboratory, the original model skeleton is scaled using the precise placement of the reflective markers so that the patient's geometry can be captured accurately [51]. These models are used to create simulations of movement to allow the study of different neuromuscular conditions, analyze athletic performance, and estimate muscle and joint loading of the musculoskeletal system [52].

Figure 2:

Overview of the forward dynamics approach to neuromusculoskeletal modeling to estimate muscle forces and joint moments given the neural signal (EMG) [50].

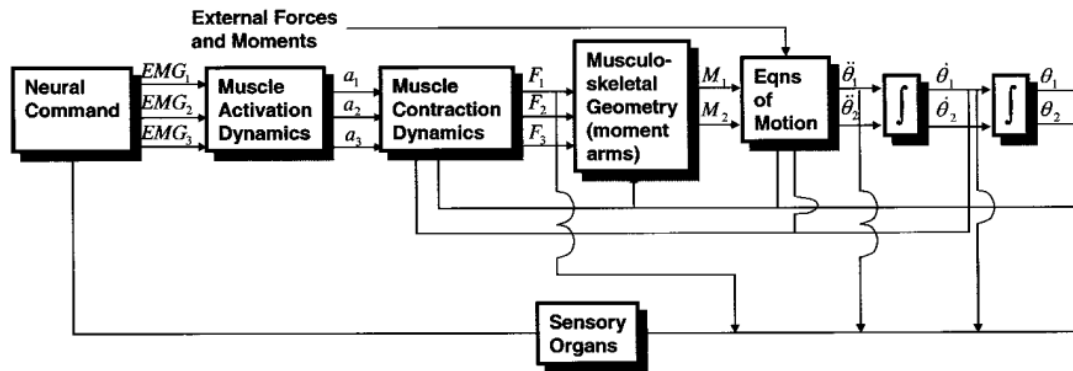
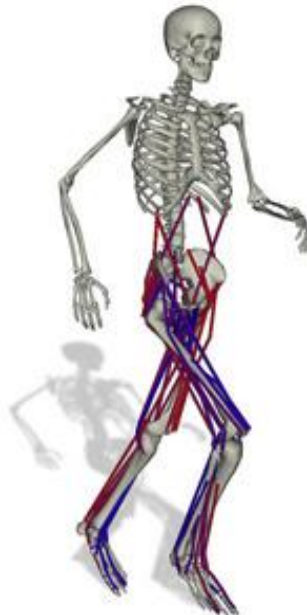


Figure 3:

Example of a NMS model of the lower extremities created in OpenSim [52].



CHAPTER 3: PRIOR WORK

3.1. Prior Work: Subject-Specific Muscle Synergy Model

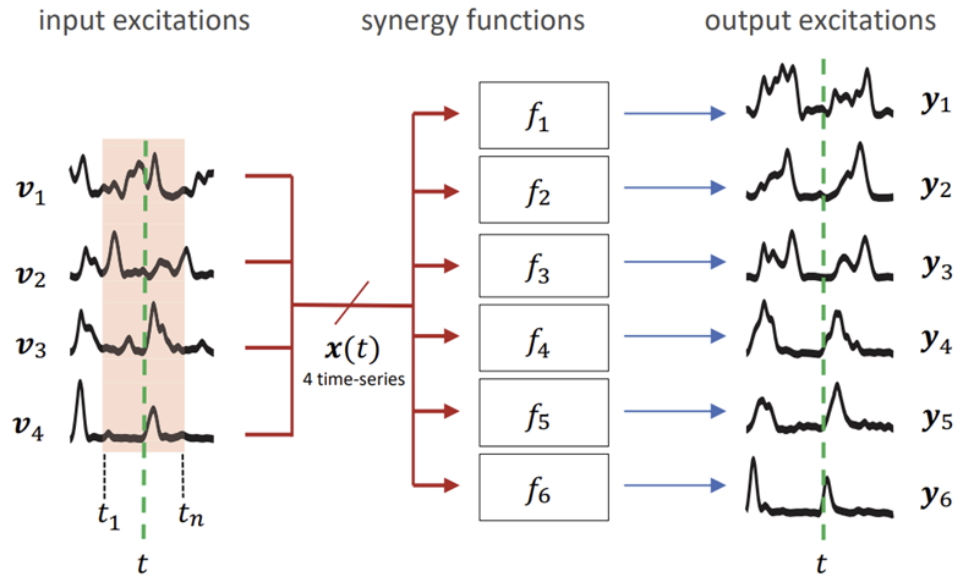
Advanced machine learning techniques such as regression have been utilized as a means to reduce the number of electromyography sensors necessary for estimating muscle activation time-series data [37,38]. Regression models are developed from a large number of inputs and observations and can be viewed as a function approximation problem, such that a function among a well-defined class approximates a target function in a task-specific way [53]. Regression techniques have the ability to capture the relationship between wearable sensor inputs and biomechanical time-series outputs.

Gaussian Process Regression (GPR) is the machine learning model that was chosen to model the muscle synergy functions. GPR is a nonparametric, Bayesian approach to regression that does well with small datasets. Covariance functions are used to define the similarity of two data points and describe how much two random variables change together (their covariance) with varying separation. Another advantage of GPR is that it models the variance of the estimate, which is suitable for wearable sensor frameworks [54].

The novel developments in [38] include the subject-specific Gaussian process model of muscle synergy functions to estimate unmeasured muscle excitations using only a subset of EMG data. Figure 4 is an overview of the muscle excitation estimation procedure. Excitations for six muscles were estimated from four muscles (called the input muscles) with a mean absolute error (MAE) less than 5% of the maximum voluntary contraction (MVC). These estimated excitations informed muscle activations with less than 4% MAE and 89-93% variance accounted for (VAF).

Figure 4:

Visual overview of muscle excitation estimation procedure from [38] where there are four measured excitations input into the synergy functions to estimate the six unmeasured output excitations.



A detailed analysis of a number of different modeling choices was also examined by testing every possible combination of four-, three-, and two- muscle input sets. The best muscle input sets were determined by which combinations of muscles had the stronger correlations ($r > 0.67$) compared to the rest of the possible combinations. Other performance statistics (RMSE, VAF, etc.) were also considered [38] in ranking input muscle sets. The performance of the Gaussian process stationary covariance function (squared exponential) and non-stationary one were also compared - the stationary one performed better in almost all aspects so only that was included in the analysis. Lastly, the relationship between window size and performance was investigated. Window size is the

length of the sliding cutout of a time sequence of data. The best input window structure and muscle input sets were determined using a custom heuristic (z-score averaging method [38]) for ranking different models.

3.2. Gap Analysis

In this thesis, I advance the use of muscle synergy functions by creating subject-general models, which leverage the synergistic relationship within a group of muscles, to reduce the complexity of wearable sensor arrays and overcome the current need for an in-person visit to a human performance laboratory for calibration. This is a continuation of the current subject-specific [38] approach. In a recent systematic review, most studies present subject-specific models (80%) and 33% of studies explored task extrapolation [37]. Subject-general models have the potential to generalize performance across healthy and impaired populations. This thesis contributes to the research needed to better understand how these regression models generalize across individuals in a task-specific way (walking) [55].

Subject-specific models require in-person calibration activities that limit their use. Additionally, compared to subject-specific models, subject-general models generalize better across populations. Many studies suggest that the eventual users of their remote monitoring systems are expected to be people with clinical impairment [37]. However, training a subject-specific model on a person who cannot properly activate their muscles may impact the training efficacy of the model. A subject-general model could then instead be trained on a spectrum of levels of impairment for any given clinical population.

Whenever data collection sessions occur in the lab, the instrumentation process can take up to an hour. However, it is known that when we are doing our own palpations and placement, and checking for good signal quality, we're going to get good high quality data. Challenges we currently face collecting this data includes the need for lots of sensors. New approaches that can provide the same quality data but with less sensors to simplify the process and save time are necessary, as data collected in laboratory-controlled settings are often not a good representation of how someone truly moves during their daily life. Patients are more motivated to wear sensors when it doesn't impact their daily life and is easy to manage/incorporate into their daily routine. The complete set of measured and estimated excitations could be used to drive EMG-driven forward dynamics to compute muscle and joint loading. Wearable sensors that someone can wear at home combined with subject-general models are part of the solution to this.

3.3. Defined Aims

The goal of this thesis is to reduce the number of wearable sensors required for remote monitoring of joint and muscle loading by creating subject-general muscle synergy models using Gaussian process regression to replicate the performance of the current subject-specific approach and fulfill the gaps stated above.

This objective can be further specified by the following:

1. Compare the performance of the subject-general models against the current subject-specific approach.
2. Explore the effect of adding kinematic data to the model.

These two aims will be discussed further in Chapters 5 and 6 and have the potential to advance wearable-sensor based remote gait analysis techniques and performance monitoring. Both utilize new approaches for estimating unmeasured muscle excitations using only a subset of EMG data.

From prior work, it is known that a higher amplitude of a gyroscope signal (angular velocity magnitude) is associated with the swing phase of the gait cycle [56]. Providing the model with information about what phase of the gait cycle the subjects are in provides additional information to solve the function approximation problem. Different muscle synergies are activated at different phases of the gait cycle because someone has to recruit different muscles for each individual movement during walking. Providing the model with this information is another way for it to learn which synergies, and thus muscles, may or may not be activated at a given time. When the angular velocity magnitude is of interest, gyroscopes do not require precise placement on a patients' part, so the combination of fewer EMG sensors combined with the addition of gyroscope sensors make for practical remote deployment.

CHAPTER 4: DATA METHODS

4.1. Participants and Data Collection

Data were collected from a total of sixteen healthy subjects (55% male, age: 21+/- 1 years) in the motion capture lab at the University of Vermont. The goal of the study was to build a dataset characterizing human movement of healthy persons performing various activities of daily life. The study was approved by the University of Vermont Institutional Review Board (#18-0518). Participants for this study were recruited from flyers posted around the community and at the University of Vermont. To be eligible for the study, participants had to be between the ages of 18 and 50 with no history of injury or neurological disorder affecting mobility or balance and had to be able to perform typical daily activities without assistance.

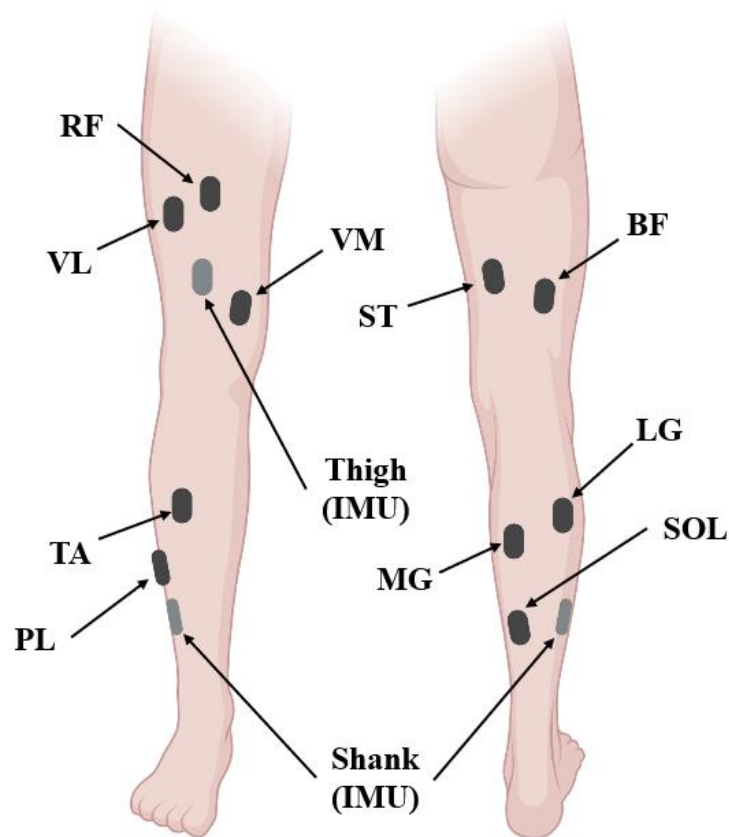
Participants were brought into the motion capture laboratory and provided written consent to complete an array of tasks. Surface electromyography (sEMG) data (BioStamp nPoint, MC10, Inc., sampling frequency: 1000 Hz) were continuously recorded from 10 muscles on the right leg: tibialis anterior (TA), peroneus longus (PL), lateral gastrocnemius (LG), medial gastrocnemius (MG), soleus (SOL), vastus medialis (VM), rectus femoris (RF), vastus lateralis (VL), biceps femoris (BF), and semitendinosus (ST). Electrode placement was according to SENIAM recommendations [57]. Inertial Measurement Units (BioStamp nPoint, MC10, Inc., sampling frequency: 1000 Hz) continuously recorded angular velocity from the thigh and shank. Sensor locations are illustrated in Figure 5.

Participants performed several muscle-specific maximum voluntary contraction (MVC) trials and walked for one-minute at a self-selected walking speed on a level

treadmill. The average walking speed was 0.84 ± 0.13 m/s and the average stride time was 1.31 ± 0.22 s. Following a visual sEMG signal quality check, all data for seven subjects were removed as there was no clear signal during walking for at least one muscle and only the nine subjects remaining with the highest quality EMG data were used in the analysis.

Figure 5:

Anatomical diagram of EMG and IMU sensor placement locations on cartoon leg on the front (left) and back (right) view of the right leg. IMU sensors are illustrated in light grey and EMG sensors are illustrated in dark grey with corresponding labels of the sensor location names.



4.2. Signal Processing Techniques

4.2.1. Electromyography Signals

Muscle excitations were computed from raw sEMG data using methods common for estimating muscle force [29]. Data were digitally high-pass filtered at 30 Hz to remove low frequencies and any vertical shift in the data, rectified to produce a positive signal, low-pass filtered at 6 Hz to remove high frequency noise, and normalized by the maximum value across the walking trial and maximum voluntary contraction (MVC) trials, where it is represented as a percentage of the maximum effort contraction. All muscle excitation time-series were initially resampled to 250 Hz in Chapter 5 and further resampled to 100 Hz to reduce the number of inputs to the machine learning model.

Figure 6:

Electromyography signal from a subject's medial gastrocnemius during walking, before filtering.

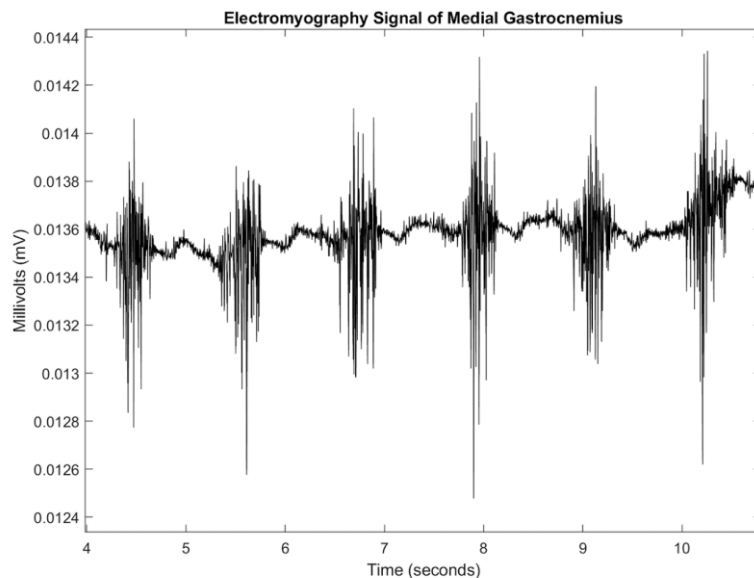
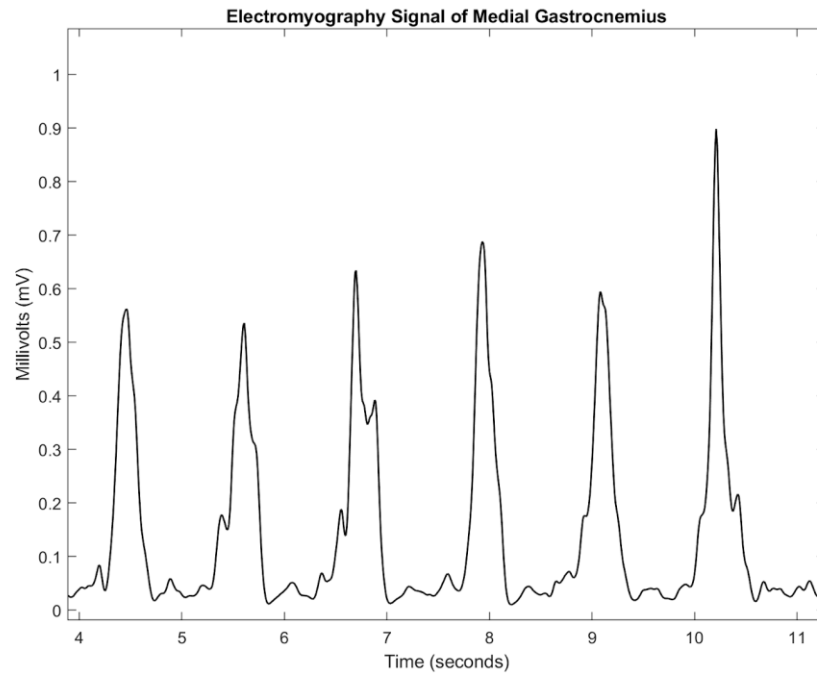


Figure 7:

Electromyography signal from a subject's medial gastrocnemius during walking, after filtering.



4.2.2. Gyroscope Signals

The magnitude of the angular velocity signal was calculated, low-pass filtered at 6 Hz, and normalized to compute the vectorwise z-score and rescaled to be between 0 and 1 so it is scaled similarly to an EMG signal after it is filtered. All angular velocity signals were resampled to 100 Hz to reduce the size of the model input structure.

Figure 8:

Gyroscope signal from a subject's lower leg (shank) segment during walking, before filtering.

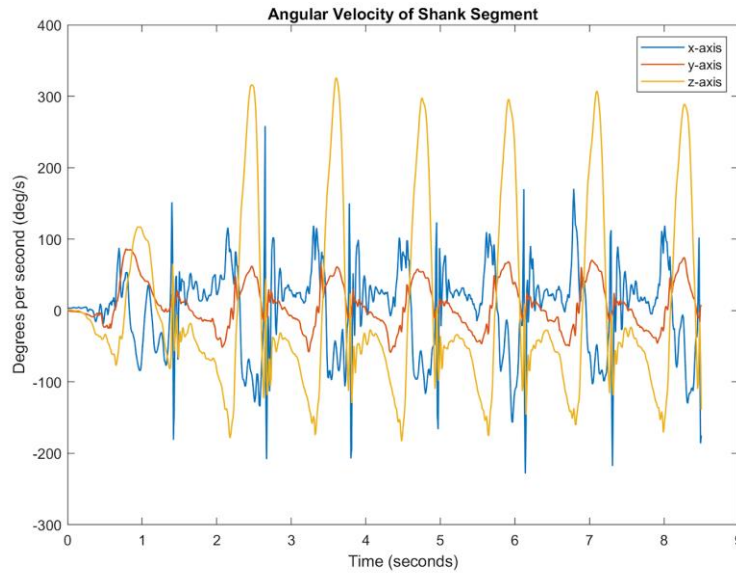
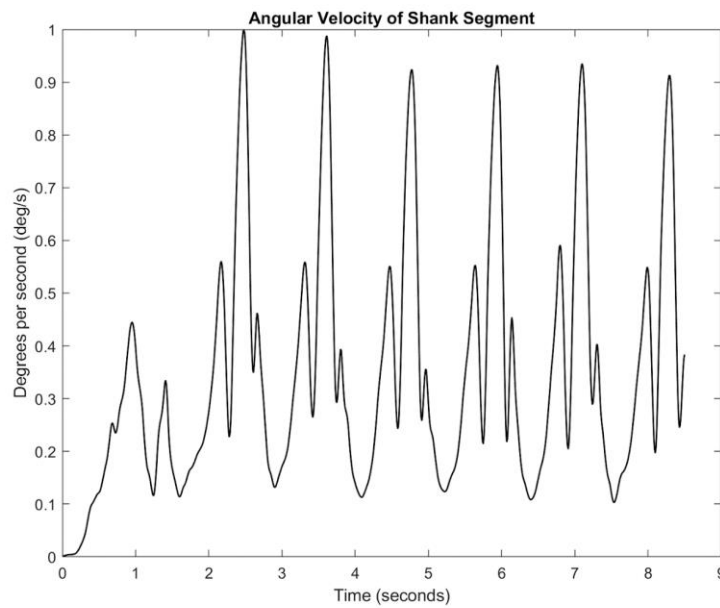


Figure 9:

Gyroscope signal from a subject's lower leg (shank) segment during walking, after filtering.



CHAPTER 5: SUBJECT-GENERAL MUSCLE SYNERGY MODELS

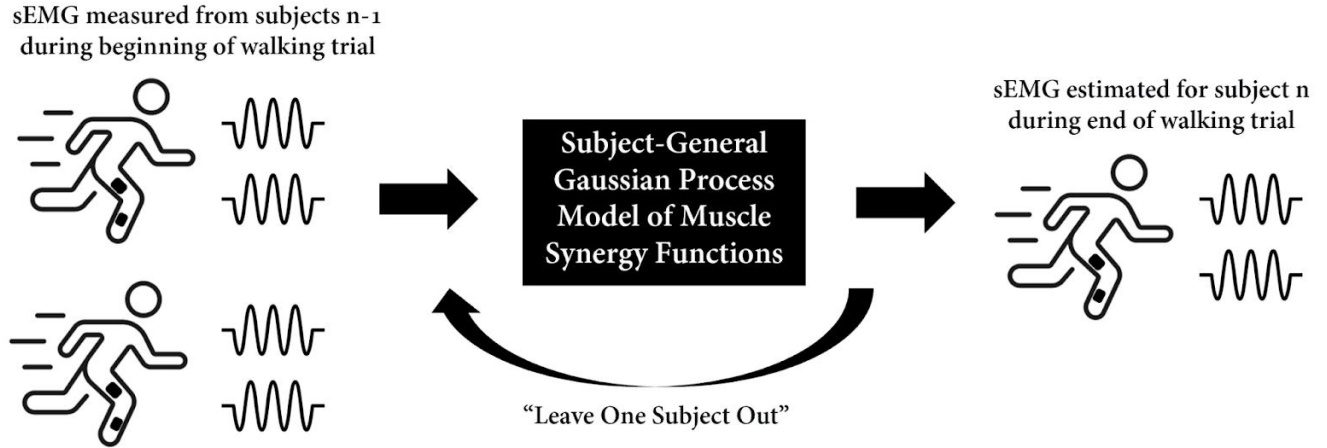
5.1. Problem Statement

The objective of the first aim is to compare the performance of the subject-general models against the current subject-specific approach. Compared to subject-specific models, subject-general models generalize better across populations because they are not person-specific, such that all of the data used to train and test a given model are taken from the same subject. This initially requires full instrumentation and in-person calibration activities in order to deploy it remotely. For impaired populations such as people with MS, HD and PD who rely on a caregiver and those living in rural or underserved areas, this visit might not be feasible. With subject-general, the model would be able to be trained across a range of functional levels of impairment so it could capture a broader spectrum of any given disease population.

Figure 10 is an overview of the leave-one-subject-out method for training and testing a subject-general model. The subject-general model has a similar framework to the subject-specific model in that it is trained on data from the beginning of the walking trial and tested on data from the end. The difference is that it is trained on data from every subject except one, and that is the one it is tested on. This is also known as “leave one subject out” and it will iterate as many times as there are subjects. This analysis is task specific and muscle specific and will focus solely on a walking task.

Figure 10:

Visual overview of how the subject-general model works.



5.2. Methods

For the first aim, a direct comparison of the general model was to be made to the specific model, so it was important to keep as many other factors as possible the same as in [38]. Hyperparameters such as stopping criteria and downsampling frequency were kept fixed. The window size, input muscle sets and covariance function which were identified as optimal were used.

The script used to train and evaluate the model was reconfigured so it would accept multiple inputs across a user-defined number of subjects instead of just one. It was validated to be working properly by including 2 copies of the same subject for the model to be trained and tested on. The model's performance was close to perfect, which was to be expected. It is important to note that this analysis was solely for testing that the changes made were working properly and was not included in the final results.

The subject-general model was tested on nine subjects for the best 4-, 3-, and 2-input muscle sets. For the four-muscle input set, which would be the BF, PL, SOL, and VL to estimate the MG, LG, TA, ST, VM and RF. The three-muscle input model used the BF, PL, and SOL to estimate the MG, LG, TA, ST, VM, RF and VL. Lastly, the two-muscle input model used the LG and SOL to estimate the MG, TA, ST, VM, RF, BF, PL and VL. Chapter 4 describes the data collection and signal processing methods. All EMG signals were downsampled to 250 Hz to reduce the sample size and explore the performance of the data for frequencies commonly used in remote monitoring. The input window size was set to 1500ms as specified, which represents the size of the sliding window. The number of functional iterations (i.e. stopping criteria) was set to 50 iterations [54]. In some cases, muscles being evaluated were able to reach true minima before 50 iterations were completed. Lastly, the model was trained on 25% (20-45%) of data from the first half of the walking trial and tested on 25% (55-80%) of data from the second half.

The subject-general model was also tested on nine subjects for a 1-muscle input model. SOL was chosen as the single muscle input because it was the only muscle that had been included in every optimal muscle input set.

5.3. Results

The subject-general model was evaluated using four performance metrics common for evaluating biomechanical time series: Pearson's correlation coefficient (r) percentage of variance accounted for (VAF), root mean square error (RMSE), and mean absolute error (MAE). RMSE and MAE are scaled to be in units of percentage of MVC.

Each metric was computed for each muscle-specific synergy function corresponding to each muscle in the estimated set by comparing the estimated excitations with the true excitations in the test set as done in [38]. Figure 11 is an example of the performance of the medial gastrocnemius (MG) muscle synergy function for subject 1 during a 14.5 second sample of the walking trial. This muscle synergy function was chosen for individual analysis because it had the highest correlation between the true and estimated signal. The black line is the true EMG signal, and the red line is the estimated one, in millivolts (mV). The data in Table 1 are the reported outcomes for the MG muscle. The correlation (r) is 38% lower than the correlation reported for the subject-specific model.

As the number of input muscles decreases, the MG performance metrics vary. For the 2-muscle input model, r increases so it is only 31% lower than the subject-specific model. The results of the 3-muscle model and there was a 35% difference. Lastly, for the 1-muscle model (including the SOL only), r was reported to be 0.55, equivalent to the 4-muscle model.

Figure 11:

Results of the true vs. estimate signal of the MG muscle for the 4-muscle input model for Subject 1.

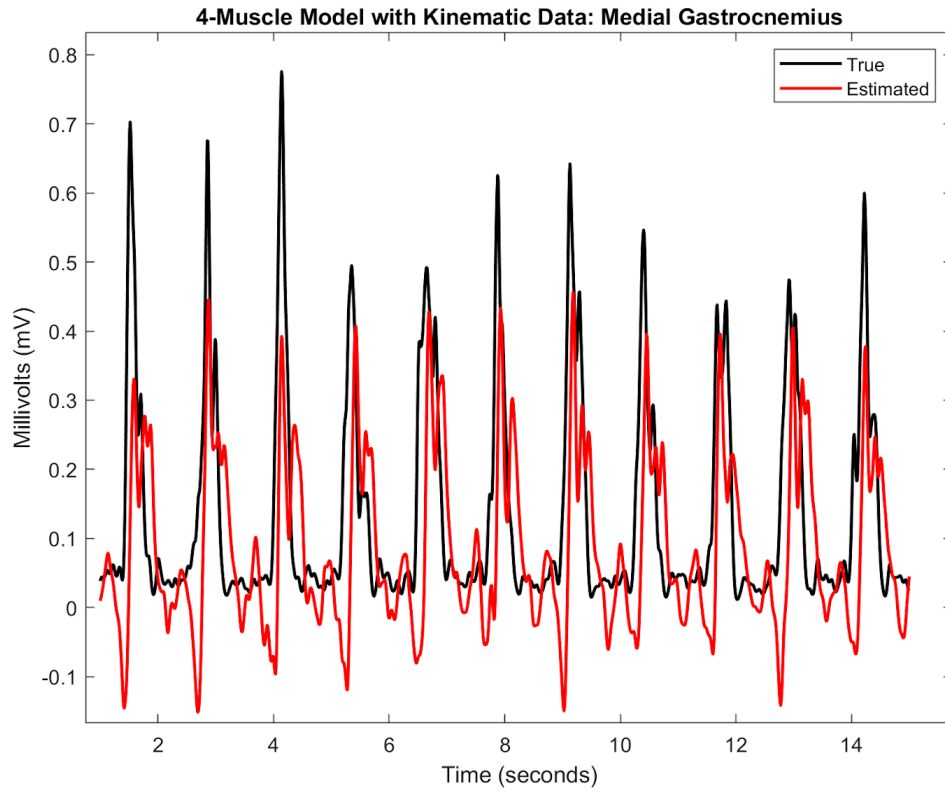


Table 1:

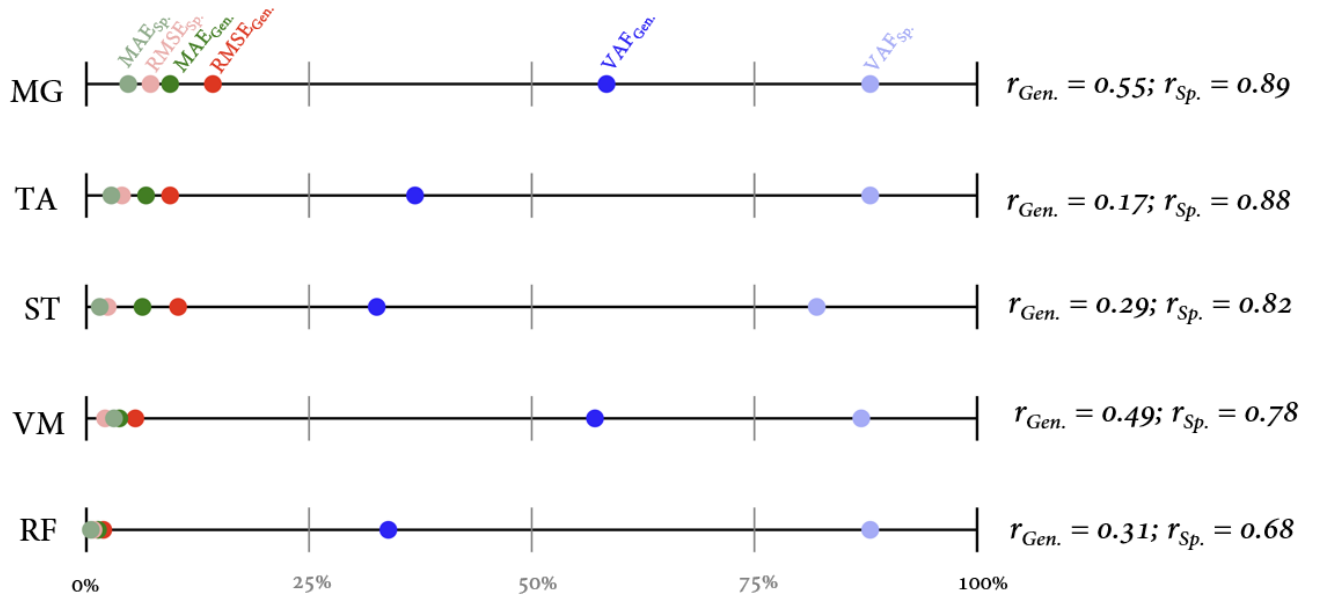
Summary statistics for MG muscle for 4-, 3-, 2-, and 1- muscle input subject general models and the results of the subject-specific model in parentheses to compare, apart from the single muscle model.

Muscle Model	RMSE	MAE	<i>r</i>	VAF
4-Muscle Input	0.14 (0.07)	0.09 (0.05)	0.55 (0.89)	0.58 (0.88)
3-Muscle Input	0.14 (0.07)	0.09 (0.05)	0.58 (0.89)	0.61 (0.87)
2-Muscle Input	0.13 (0.06)	0.09 (0.04)	0.64 (0.91)	0.66 (0.9)
1-Muscle Input	0.14	0.1	0.55	0.59

Figure 12 is a summary of the statistical results for the 4-muscle input model across all subjects for each muscle excitation that was estimated and how they compare to the subject-specific results. These five muscles were commonly estimated across all muscle input sets, so they were chosen to be used to analyze results across different models. The reported VAF, RMSE, and MAE values are the average across all subjects for each muscle. The darker hue is the results averaged across all subjects for the subject-general model, and the lighter hue is the specific model with *r* on the right-hand side for context.

Figure 12:

Visual summary of the statistical results for the 4-muscle input model across all subjects for each muscle excitation that was estimated and how they compare to the subject-specific results (RMSE and MAE values are expressed in units percentage of MVC).



5.4. Discussion

With the need for a way to reduce the complexity of wearable sensor arrays and conduct muscle and joint loading studies remotely, the results presented above suggest that methods similar to these could fulfill that need. In Figure 11, it can be seen that the muscle activation peaks are lower for the estimated signal than the true signal, however this is useful for clinical purposes because the estimated signal could then be used to detect activation at specific timing because the peaks are clear and identifiable.

The MG muscle was chosen to compare across models in Table 1 because it is activated at every step in a healthy population. It can be seen that the MG has the strongest correlation between the true and estimated signal in the 2-muscle input set ($r = 0.64$). This was true for the specific model as well. Aside from the MG, most correlations decreased as we introduced a smaller number of muscles into the input muscle set. The SOL was chosen for the 1-muscle input set because it is the only muscle that was included in every other input muscle set. The statistical characteristics show promising results as the correlation between the true and estimated signal was equivalent to that of the 4-muscle model ($r = 0.55$) and it should be explored more using other muscles. In Figure 12, it was common for the VAF to have the greatest difference between the general and specific models. In literature, subject general models appear to frequently result in performance decreases [58,59]. This may indicate that the modeling or data sampling techniques may need to be investigated further.

Different selection criteria for the input muscle sets may be considered for future work. The results for the MG muscle support that there is a way to systematically choose muscles that are close in proximity to the ones we are interested in estimating. I believe the MG muscle's performance was better for the 2-muscle input set because it was the only model that included the LG muscle, which is close to the MG and contracts at similar timing. This could also be done by choosing muscles based on what we know about different muscle characteristics in humans such as PCSA and the pennation angle. The muscles chosen should also change depending on the activity. This information could be

used to inform the future work of exploring a single muscle model in combination with kinematic data.

In conclusion, these results are promising for the deployment of technologies used to estimate muscle forces and joint loading, such as the one discussed in Chapter 7, meeting rural healthcare needs and driving neuromusculoskeletal modeling.

CHAPTER 6: EFFECT OF KINEMATIC DATA

6.1. Problem Statement

The objective of the second aim is to explore the effect of adding kinematic data to the model in addition to the electromyography data. As discussed in Chapter 3.3, from prior work it is known that a higher amplitude of a gyroscope (angular velocity) signal is associated with the swing phase of the gait cycle. Figure 13 on the right is a concept plot of the shank segment angular velocity in deg/s with the stance and swing phase highlighted, and a visualization of the thigh, shank and foot segments to illustrate the direction the limb is moving on the left [60]. It is important to note that the angular velocity from the thigh segment and shank segment are going to differ. Angular velocity of the shank segment is the most positive mid-stance phase and the most negative mid-swing phase. Figure 13 also includes a depiction of what the vertical ground reaction force would look like in walking. The points at 0% and 60% gait cycle represent the heel-strike and toe-off events respectively. Acceleration happens just after the toe-off event when the foot starts to accelerate in the forward direction, and mid-swing occurs when the foot passes the contralateral foot. Deceleration happens just before the starting of the next cycle when muscles prepare to stabilize the foot on the ground [61]. Figure 14 is an example of 3 strides measured from the shank segment with the stance phase labeled in blue.

Figure 13:

Conceptual plot of the lower limb segment angular velocity during stance and swing phase [60].

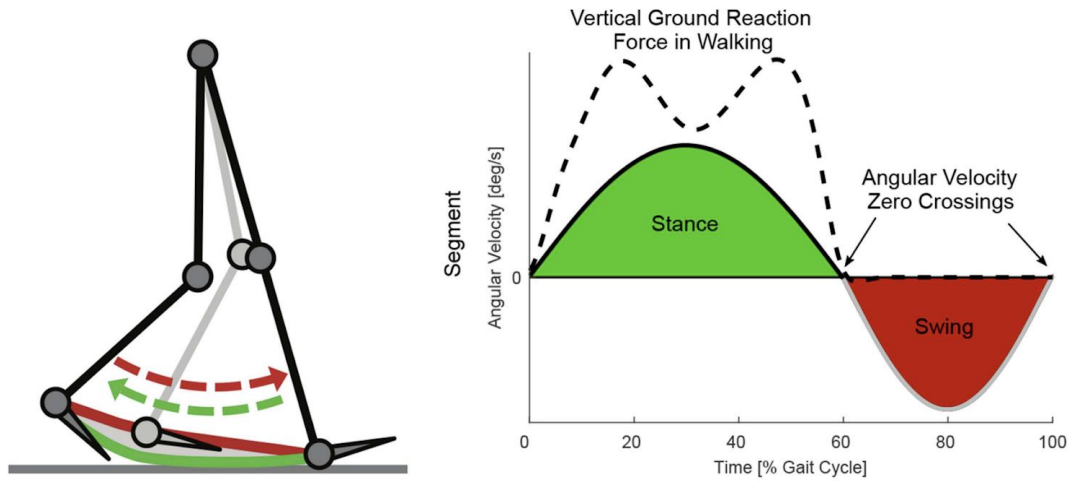
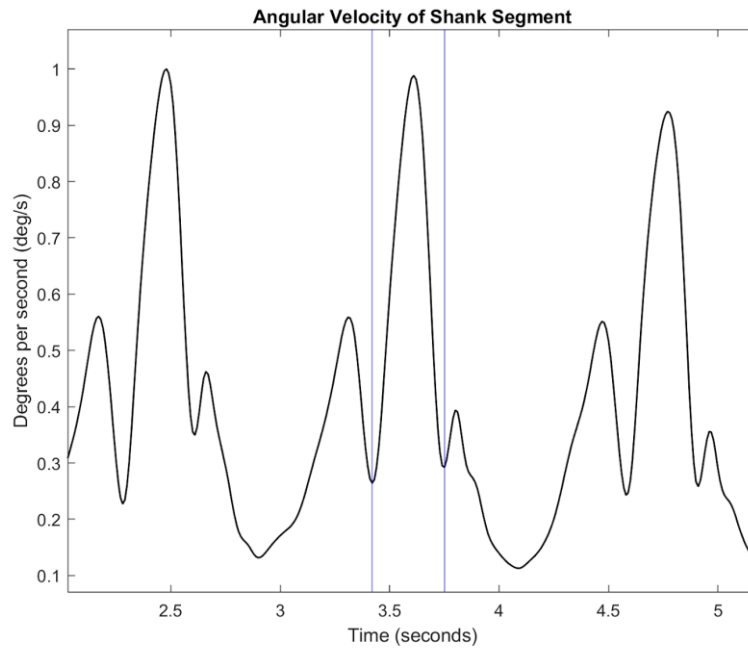


Figure 14:

Angular velocity of the shank segment during three walking strides with the peak angular velocity between two blue lines which highlight swing phase.



In Chapter 5, the goal was to directly compare to results reported in [38] so no changes were made to the model hyperparameters. In this aim, parameters are tuned to achieve better performance than the subject-general models without kinematic data under the same conditions.

6.2. Methods

For the second aim, the goal was to observe the effect adding kinematic data to the subject-general model had on the results and use that information to tune the hyperparameters and increase the performance compared to the subject-general model without kinematic data in the training set. A new data importer and processor had to be created so raw data from the electromyography and gyroscope sensors could be loaded and processed separately. Data were processed as described in Chapter 4.2.

For the initial analyses, a 5-subject subset of the full dataset was used so the model didn't take as long to run. The subject-general model was tested using the leave-one-subject-out method as described in Chapter 5 on five subjects, then nine subject, for the 4-muscle input set (including kinematic data) only which includes the BF, PL, SOL, VL, shank and thigh gyroscope signals to estimate the MG, LG, TA, ST, VM and RF. It is important to note that the kinematic data was to never be included in the unmeasured muscle set because we are not interested in predicting gyroscope signals. The window size was kept constant throughout each analysis because 1500 ms allows the model to see an additional half stride at the beginning and end of the gait cycle for predicting the current excitation. Lastly, the model was trained on 50% (10-60%) of data from the first half of

the walking trial and tested on 25% (65-90%) of data from the second half to include more data in the training set.

Dataset reduction techniques were explored to increase processing speed and overcome computer memory challenges. Until this point, all signals were being downsampled to 250 Hz. This was further reduced to 100 Hz as mentioned in Chapter 4. As discussed in Chapter 5, the number of functional iterations (i.e. stopping criteria) was set to 50 iterations and in some cases, muscles being evaluated were able to reach true minima before 50 iterations were completed. Given the changes described above, this was no longer the case and it had to be increased multiple times. The number of observations represents the maximum number of observations the dataset is reduced to in the training set. It was initially thought that reducing the number of gyroscope sensors to solely the shank and increasing the observations as much as possible would yield the best performance. This also indicated the original number of observations was now too small for the number of inputs the general model has now. Additionally, models including both gyroscope sensors performed better than only the shank, so both gyroscopes were used in the final analyses. Reducing the sampling frequency to 100 Hz allowed for the optimal number of observations for this dataset to be identified and number of iterations to be maximized without decreasing the processing speed.

The performance of the subject-general model including kinematic data in the training set with the new parameter settings were compared against the performance of the subject-general model without kinematic data under identical conditions before moving to the full dataset.

6.3. Results

The subject general models were evaluated using four performance metrics described in Chapter 5. As discussed in Chapter 6.2, dataset reduction techniques were explored to identify the optimal parameters for the 5-subject and 9-subject model, with and without kinematic data. Table 2 describes samples of the 5-subject trials taken to determine 12000 observations was the optimal number of observations for this dataset. Each column is a trial and each row is a parameter where either the number of gyroscope sensors used, observations or iterations were varied. Trial 1 is equivalent to the settings in Chapter 5 and [38]. The downsampling frequency was decreased to 100 Hz as per the dataset reduction techniques so that the number of observations could be increased to 15000. Only the shank data was utilized while testing these parameters to further reduce the number of inputs into the model. After observing a decrease in performance between Trial 2 (15000 observations) and Trial 3 (18000 observations), 12000 observations were tested and proven to yield better results than Trial 1. Adding the Thigh gyroscope data and increasing the number of iterations also increased the performance in Trial 4. It was concluded that for the number of observations, increasing past 12000 observations reduced the performance and using data from both gyroscope sensors achieved the best results.

Table 2:

Comparison of different parameter settings for 5-subject, 4-muscle input model after the addition of kinematic data.

Parameters	Trial 1	Trial 2	<i>Trial 3</i>	Trial 4
Gyroscope Sensors	Thigh & Shank	Shank Only	Shank Only	Thigh & Shank
Iterations	100	100	110	110
Observations	7500	15000	18000	12000
Downsampling Frequency	250 Hz	100 Hz	100 Hz	100 Hz
Average Correlation	44.2%	37.6%	36.6%	47.2%

For the 5-subject model, muscles being evaluated were able to reach true minima after increasing to 110 iterations in Table 3. However, this was not the case for the 9-subject model. Table 3 describes samples of the 9-subject trials taken to test how many iterations were necessary to reach true minima for this dataset. After testing 150 and 200 iterations in Trials 5 and 6 respectively, most muscles being evaluated were able to reach true minima. To increase the number of iterations even further, more computing power was required. For Trials 7 and 8, a workstation computer was used to run the program instead of a laptop. The highest average correlation reached for the 9-subject model before this point was 39.3%. After increasing the downsampling frequency to its original settings, the performance increased slightly to 40.2%. All muscles being evaluated were able to reach true minima in Trial 7, however this was not the case for Trial 8 which indicates the number of iterations should be further increased in future work.

Table 3:

Comparison of different parameter settings for 9-subject, 4-muscle input model after the addition of kinematic data.

Parameters	Trial 5	Trial 6	Trial 7	Trial 8
Gyroscope Sensors	Thigh & Shank	Thigh & Shank	Thigh & Shank	Thigh & Shank
Iterations	150	200	500	500
Observations	12000	12000	12000	12000
Downsampling Frequency	100 Hz	100 Hz	100 Hz	250 Hz
Average Correlation	39.3%	39.3%	39.3%	40.2%

The highest correlation among all the 4-muscle input subject general models was that of the 5-subject model with kinematic data in Trial 4. As more subjects were added, the performance decreased in Table 3. This was to be expected because more data requires more evaluations for the solution to be optimal.

Figure 15 is a summary of how the different kinematic model parameter settings for the 4-muscle input model influenced the performance compared to an identical model without kinematic data. Each line represents a model tracing the number of iterations and observations from left to right, landing on the average correlation for across all muscles estimated. The downsampling frequency was set to 100 Hz for each model and everything was trained on 50% of the data from the first half of the walking trial.

Figure 15:

Visual summary of the performance of the 4-muscle input model with varying parameters (number of iterations, observations, and subjects) to describe how the affect performance (average correlation across all of the estimated muscles, expressed as a percentage).

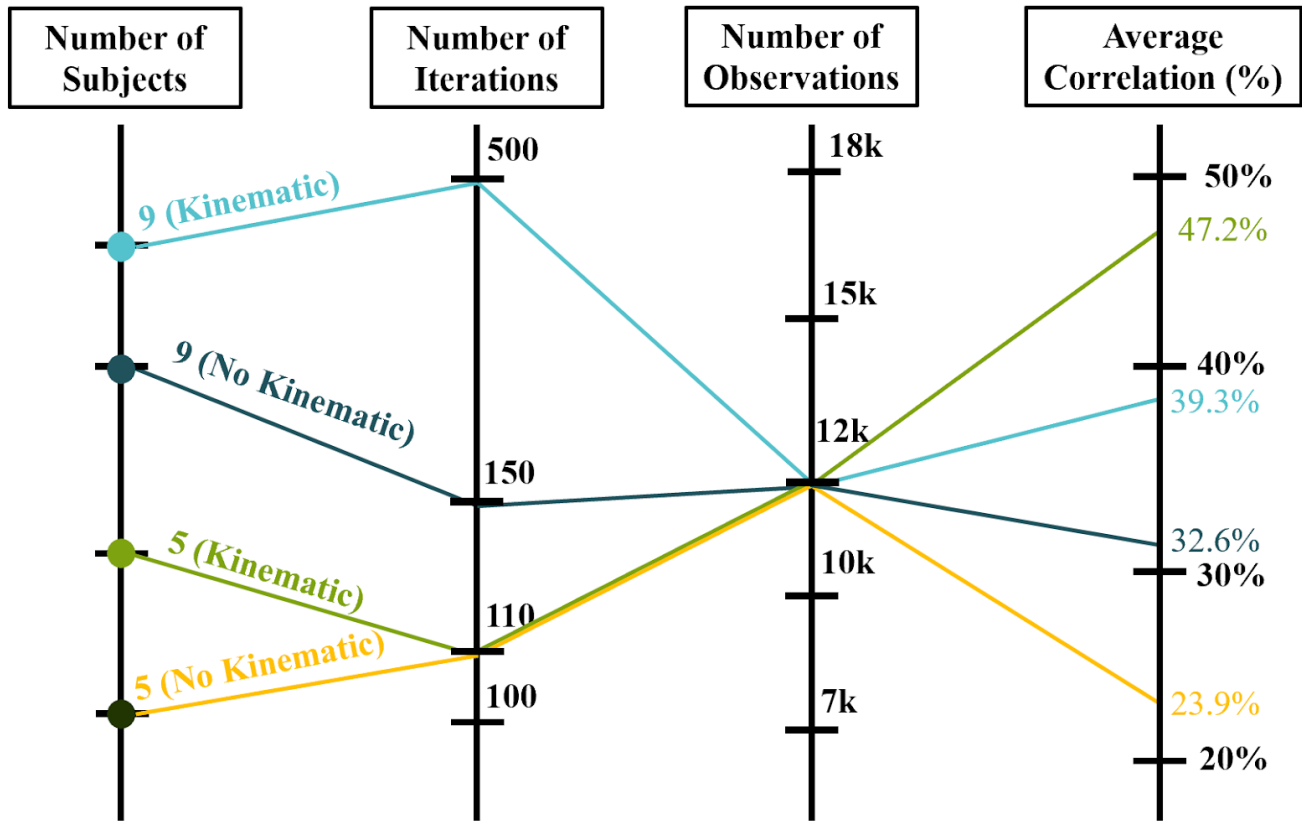


Table 4 describes the statistical performance of the kinematic model (left) against the model without kinematic data (right) across all muscles for the 9-subject, 4-muscle input model. For all six muscles, improvements can be seen when kinematic data is included. The highest improvement in correlation can be seen for the ST muscle with a 50% improvement in correlation. Following that is the TA which saw a 42% improvement.

The RMSE and MAE metrics appear to be very similar between both models. It is important to note that the ST muscle consistently performed poorly, which may indicate the data collected was not good data and may be causing the program to run longer. The variance accounted for (VAF) represents how far each estimated excitation is from the mean of the true excitation. There does not appear to be a clear trend whether including kinematic data reduces the variance or not, however, it improves the performance for the ST model.

Table 4:

Comparison of the summary statistics between the kinematic (kin.), i.e. Trial 7 and no kinematic (no kin.) 9-subject, 4-muscle input subject general model.

Muscle	RMSE		MAE		r		VAF	
	Kin.	No Kin.						
MG	0.11	0.11	0.07	0.07	0.42	0.34	0.48	0.48
TA	0.07	0.08	0.05	0.06	0.45	0.26	0.56	0.48
ST	0.11	0.11	0.07	0.07	0.10	0.05	0.16	0.19
VM	0.05	0.05	0.03	0.03	0.54	0.49	0.59	0.58
RF	0.02	0.02	0.01	0.01	0.30	0.28	0.48	0.40
LG	0.11	0.11	0.07	0.07	0.42	0.34	0.48	0.48

The average correlation between true and estimated excitations was 96% higher when angular velocity data was included in the 5-subject, 4-muscle input model set as

illustrated in Figure 15. The estimated excitations informed muscle activations with 6.7% mean absolute error (MAE) and 43% variance accounted for (VAF) averaged across all muscles when kinematic data was included in the model, and 7.3% MAE and 43% VAF without kinematic data. These results lay the groundwork for developing muscle synergy functions that no longer require in-person calibration, paving the way for completely remote studies of muscle and joint loading.

6.4. Discussion

There are many advantages to exploring the use of kinematic data in remote gait analysis. When the angular velocity magnitude is of interest, gyroscope sensors do not require precise placement like EMG sensors because vector magnitudes are unchanged under pure conditions. In theory, the angular velocity of a rigid body such as the shank segment is the same about every point in that body. So, a gyroscope placed distally on the shank near the ankle and a gyroscope placed proximally on the shank near the knee should render the same measurement. Gyroscopes are often embedded in smartphones which would be ideal for some remote studies. Because of this, these sensors are more easily integrated into clothing. However, gyroscope sensors also have high power requirements that would limit long-term capturing.

When tuning these parameters, it was interesting to see how much effect each of them had on the excitation estimates. As shown in Figure 15 when increasing from 5 to 9 subjects, the more data that is included the more iterations are required and the longer it will take. This makes sense because the more data a model is given, whether it is from more subjects or additional sensors, the longer the synergy functions take to optimize. This

is not efficient for deployment purposes and revealed limitations. Downsampling techniques should be investigated further to be able to run the models more efficiently on a local machine and be able to compete with the performance of the subject-specific model. This could be done by exploring a new modeling approach or a new way of sampling data.

In Figure 15, all muscle estimates reached true minima under those conditions so the different models could be compared to each other. However, this did not seem to change the average correlation found between 150, 200 and 500 iterations reported in Table 3. This is a known issue with GPR and large datasets and changing the model type may be a possible solution to this problem. Upon increasing the sampling frequency in Trial 8, it was found that the results improved slightly but would require even more than 500 iterations to reach true minima and achieve a comparable estimate. This would require more time or more processing power. I believe this should be explored in future work to ensure the evaluations reach true minima. Additionally, certain muscles that consistently perform poorly should be reevaluated for future work. It is possible that the ST muscle lacks sensitivity and causes the optimization to take longer.

In conclusion, kinematic data improves the performance of the subject-general model, but not enough to conclude that it is the only change that should be made in future work. Single and double limb support looks different in impaired populations, so including this additional info may be necessary when deploying subject-general models in clinical populations with neuromusculoskeletal diseases.

CHAPTER 7: FUTURE WORK

7.1. Future Work

As discussed in Chapters 5 and 6, future work should focus on addressing the limitations of the subject-general model so its performance is on par with the subject-specific model. It is known that for GPR models, more data will take longer to optimize [37]. More data and a larger population of data are required to increase the validity and further develop the use of these subject-general muscle synergy machine learning models. Thus, I believe future work should include exploring different modeling approaches, investigating how to learn muscle synergies, and performing hyperparameter optimization through machine learning [37,38,62,63].

In a recent systematic review, most studies present subject-specific models (80%) and are not validated on impaired populations [37]. Future work should also focus on validating these algorithms in impaired populations such as PwMS. It cannot be assumed that a model trained and tested on impaired participants will have identical performance characteristics as the same model trained and tested on healthy participants. To make these algorithms more practical for deployment, it may also be suggested that a task general model be explored, as the models presented in Chapters 5 and 6 used walking trials only. For practical deployment, the SOL and PL muscles are not considered to be the best muscles to include in the input muscle set because they are difficult to palpate. I believe SOL was usually included because it was hardest to estimate. I also think a new way of sampling data that would allow for a higher downsampling rate should be explored.

The stance phase makes up approximately 60% of the gait cycle. The swing phase of gait begins when the foot first leaves the ground and ends when the same foot touches the ground again. The swing phase makes up the other 40% of the gait cycle [60,64]. Including percentage of gait cycle as an additional input into the model should be explored in future work because it can capture certain gait events like heel strike and toe-off. Lastly, subject-general models should be validated on groups of patients with very similar and dissimilar musculoskeletal physiology to explore how common physiology affects performance. The dataset used in these analyses, height and weight were known but were not used as a factor to determine which subjects were included. Certain characteristics among different groups of people with certain physiologies could be used to inform modeling choices.

7.2. Joint and Muscle Monitoring System (JAMMS)

7.2.1. Motivation

Knee injuries are on the rise. The anterior cruciate ligament (ACL) together with the posterior cruciate ligament is the central stabilizer of the knee. It stabilizes the tibia against increased anterior translation and internal rotation [65]. The ACL is the most commonly injured ligament of the knee. The annual reported incidence in the United States alone is approximately 1 in 3500 people [20]. However, data may be underrepresented as there is no standard surveillance. The decision to undergo operative treatment is based on many factors such as the patient's baseline level of activity, age, functional demands, and occupation. Athletes and younger individuals who are more active tend to opt for surgical repair and reconstruction. Typical ACL repairs and reconstructions include tissue grafts

[66]. A recent systematic review stated that 81% of those treated with ACL reconstruction returned to some athletic activity, 65% returned to the preinjury level of competition, and 55% of high-level athletes returned to normal play and competition. Other factors that may contribute to a lower percentage of return to play may be secondary to external factors such as fear of reinjury [67].

Approximately 50% of patients who undergo ACLR go on to develop post-traumatic knee osteoarthritis (OA) at some point in their lifetime [68]. Knee OA is characterized by the loss of joint space cartilage and increased bone on bone contact within the knee joint. Previous research suggests that altered gait biomechanics following ACL reconstruction not detected during the return to play period is responsible for this phenomenon [48,68,69].

7.2.2. Project Overview

The aim of this project is to create the “Joint and Muscle Monitoring System (JAMMS)”: a knee sleeve instrumented with wearable sensors that will be worn by a patient during their recovery. The novelty of this project is that it will be able to record and store this data outside of the laboratory. The data will be a more accurate representation of how the patient walks during their daily life than if it was collected inside the lab. This will help the patient better understand their progress and clinicians can monitor them throughout their rehabilitation period. Interventions can be made to prevent post-ACLR knee OA if necessary, without having to come into the doctor’s office. The results from this project will also be used to contribute to research on post-ACLR knee OA and help researchers better understand how ACL reconstruction affects the gait cycle over time.

This project will ultimately be the deployment of this work. Not every muscle we're interested in capturing data from will be instrumented on the sleeve, and this algorithm allows for the reduced sensor array and the ability to conduct the collection of the data remotely. The long-term goal of this project is to demonstrate how this may be applied to a specific clinical population and commercialize to athletes.

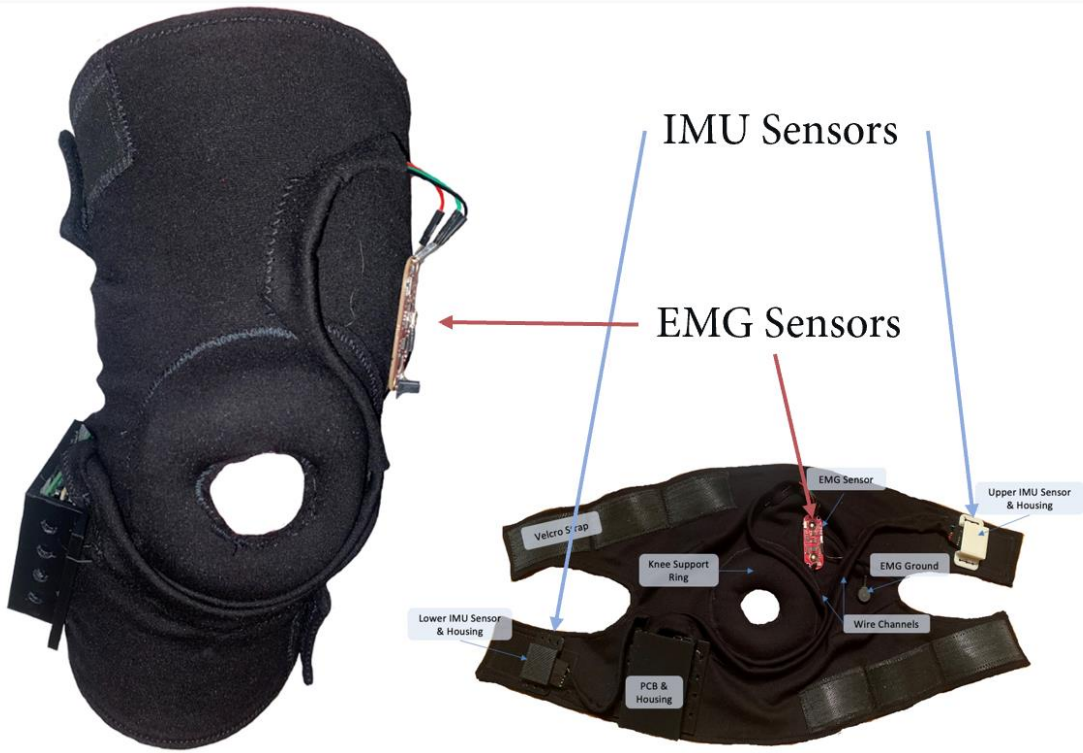
7.2.3. Evolution of JAMMS

Figure 16 is the most recent prototype of JAMMS. It is instrumented with 4 EMG sensors and two IMU sensors. In our initial customer discovery interviews, we explored two possible customer archetypes: athletes, and physical therapists. We discovered they both would benefit from having this data available and have shared frustrations when it comes to tracking rehabilitation and what to expect from the timeline when it comes to the return to sport process after injury.

My team and I were recently accepted into the academic research commercialization program at the University of Vermont and are currently working toward commercializing this project and continuing our customer discovery process. There is future work to be done on the hardware regarding the integration of wireless sensors.

Figure 16:

Latest prototype of JAMMS, a custom knee sleeve instrumented with two EMG and two IMU sensors, a PCB and battery. The IMU sensors and PCB are contained in 3D-printed casing.



CHAPTER 8: Concluding Remarks

8.1. Conclusion

In this thesis, I advance the use of muscle synergy functions to reduce the complexity of wearable sensor arrays and overcome the current need for an in-person visit to a human performance laboratory for calibration and reduce the number of wearable sensors required for remote monitoring of joint and muscle loading. The addition of kinematic data to the subject general model was shown to improve the correlation between the true and estimated excitations. These results motivate future research into the improvement of these models. Importantly, this work lays the groundwork necessary for further developing muscle synergy functions, paving the way for completely remote studies and the deployment of technologies like the Joint and Muscle Monitoring System.

REFERENCES

- [1] J. R. Morris, "Accelerometry--a technique for the measurement of human body movements," *J Biomech*, vol. 6, no. 6, pp. 729–736, Nov. 1973, doi: 10.1016/0021-9290(73)90029-8.
- [2] F. E. Zajac, "Muscle and tendon: properties, models, scaling, and application to biomechanics and motor control," *Crit Rev Biomed Eng*, vol. 17, no. 4, pp. 359–411, 1989.
- [3] Meyer, Brett M., et al. "Wearables and deep learning classify fall risk from gait in multiple sclerosis." *IEEE journal of biomedical and health informatics* 25.5 (2020): 1824-1831
- [4] Gurchiek, Reed D., et al. "Open-source remote gait analysis: A post-surgery patient monitoring application." *Scientific reports* 9.1 (2019): 1-10.
- [5] LeBlanc, Benjamin, et al. "Continuous estimation of ground reaction force during long distance running within a fatigue monitoring framework: A Kalman filter-based model-data fusion approach." *Journal of Biomechanics* 115 (2021): 110130.
- [6] McGinnis, Ellen W., et al. "Digital phenotype for childhood internalizing disorders: less positive play and promise for a brief assessment battery." *IEEE Journal of Biomedical and Health Informatics* 25.8 (2021): 3176-3184.
- [7] R. C. Klesges, L. H. Eck, M. W. Mellon, W. Fulliton, G. W. Somes, and C. L. Hanson, "The accuracy of self-reports of physical activity," *Med Sci Sports Exerc*, vol. 22, no. 5, pp. 690–697, Oct. 1990, doi: 10.1249/00005768-199010000-00022.
- [8] S. R. Fox, R. D. Gurchiek, A. T. Ursiny, B. M. Meyer, J. M. Boughton and R. S. McGinnis, "Adaptive Surface Electromyography Normalization for Long-Duration Recordings," 2021 IEEE 17th International Conference on Wearable and Implantable Body Sensor Networks (BSN), Athens, Greece, 2021, pp. 1-4, doi: 10.1109/BSN51625.2021.9507026.
- [9] G. I. Papagiannis et al., "Methodology of surface electromyography in gait analysis: review of the literature," *J Med Eng Technol*, vol. 43, no. 1, pp. 59–65, Jan. 2019, doi: 10.1080/03091902.2019.1609610.
- [10] Frechette, Mikaela L., et al. "Next steps in wearable technology and community ambulation in multiple sclerosis." *Current Neurology and Neuroscience Reports* 19.10 (2019): 1-10.
- [11] Meyer BM, Tulipani LJ, Gurchiek RD, Allen DA, Solomon AJ, et al. (2022) Open-source dataset reveals relationship between walking bout duration and fall risk classification performance in persons with multiple sclerosis. *PLOS Digital Health* 1(10): e0000120. <https://doi.org/10.1371/journal.pdig.0000120>

- [12] Tulipani, Lindsey J., et al. "Evaluation of unsupervised 30-second chair stand test performance assessed by wearable sensors to predict fall status in multiple sclerosis." *Gait & Posture* 94 (2022): 19-25.
- [13] Tulipani, Lindsey J., et al. "The sit-to-stand transition as a biomarker for impairment: comparison of instrumented 30-second chair stand test and daily life transitions in multiple sclerosis." *IEEE transactions on neural systems and rehabilitation engineering* 30 (2022): 1213-1222.
- [14] Tulipani, Lindsey J., et al. "Metrics extracted from a single wearable sensor during sit-stand transitions relate to mobility impairment and fall risk in people with multiple sclerosis." *Gait & posture* 80 (2020): 361-366.
- [15] M. Psarakis, D. A. Greene, M. H. Cole, S. R. Lord, P. Hoang, and M. Brodie, "Wearable technology reveals gait compensations, unstable walking patterns and fatigue in people with multiple sclerosis," *Physiol. Meas.*, vol. 39, no. 7, p. 075004, Jul. 2018, doi: 10.1088/1361-6579/aac0a3.
- [16] K. J. Kelleher, W. Spence, S. Solomonidis, and D. Apatsidis, "The characterisation of gait patterns of people with multiple sclerosis," *Disability and Rehabilitation*, vol. 32, no. 15, pp. 1242–1250, Jan. 2010, doi: 10.3109/09638280903464497.
- [17] C.-J. Hsu, A. Meierbachtol, S. Z. George, and T. L. Chmielewski, "Fear of Reinjury in Athletes," *Sports Health*, vol. 9, no. 2, pp. 162–167, Sep. 2016, doi: 10.1177/1941738116666813.
- [18] Gurchiek, Reed D., et al. "Remote gait analysis using wearable sensors detects asymmetric gait patterns in patients recovering from ACL reconstruction." 2019 IEEE 16th International Conference on Wearable and Implantable Body Sensor Networks (BSN). IEEE, 2019.
- [19] McGinnis, Ryan S., et al. "Wearable sensors capture differences in muscle activity and gait patterns during daily activity in patients recovering from ACL reconstruction." 2018 IEEE 15th International Conference on Wearable and Implantable Body Sensor Networks (BSN). IEEE, 2018.
- [20] S. M. Trigsted, D. B. Cook, K. A. Pickett, L. Cadmus-Bertram, W. R. Dunn, and D. R. Bell, "Greater fear of reinjury is related to stiffened jump-landing biomechanics and muscle activation in women after ACL reconstruction," *Knee Surg Sports Traumatol Arthrosc*, vol. 26, no. 12, pp. 3682–3689, Dec. 2018, doi: 10.1007/s00167-018-4950-2.

- [21] J. L. Hicks, M. H. Schwartz, A. S. Arnold, and S. L. Delp, "Crouched postures reduce the capacity of muscles to extend the hip and knee during the single limb stance phase of gait," *J Biomech*, vol. 41, no. 5, pp. 960–967, 2008, doi: 10.1016/j.jbiomech.2008.01.002.
- [22] P. B. Shull, W. Jirattigalachote, M. A. Hunt, M. R. Cutkosky, and S. L. Delp, "Quantified self and human movement: a review on the clinical impact of wearable sensing and feedback for gait analysis and intervention," *Gait Posture*, vol. 40, no. 1, pp. 11–19, 2014, doi: 10.1016/j.gaitpost.2014.03.189.
- [23] R. Takeda, S. Tadano, A. Natorigawa, M. Todoh, and S. Yoshinari, "Gait posture estimation using wearable acceleration and gyro sensors," *J Biomech*, vol. 42, no. 15, pp. 2486–2494, Nov. 2009, doi: 10.1016/j.jbiomech.2009.07.016.
- [24] T. Zimmermann, B. Taetz, and G. Bleser, "IMU-to-Segment Assignment and Orientation Alignment for the Lower Body Using Deep Learning," *Sensors (Basel)*, vol. 18, no. 1, p. 302, Jan. 2018, doi: 10.3390/s18010302.
- [25] A. Köse, A. Cereatti, and U. Della Croce, "Bilateral step length estimation using a single inertial measurement unit attached to the pelvis," *J Neuroeng Rehabil*, vol. 9, p. 9, Feb. 2012, doi: 10.1186/1743-0003-9-9.
- [26] Gurchiek, Reed D., Cole P. Garabed, and Ryan S. McGinnis. "Gait event detection using a thigh-worn accelerometer." *Gait & posture* 80 (2020): 214-216.
- [27] McGinnis, Ryan S., et al. "A machine learning approach for gait speed estimation using skin-mounted wearable sensors: From healthy controls to individuals with multiple sclerosis." *PloS one* 12.6 (2017): e0178366.
- [28] R. D. Gurchiek, N. Donahue, N. M. Fiorentino, and R. S. McGinnis, "Wearables-Only Analysis of Muscle and Joint Mechanics: An EMG-Driven Approach," *IEEE Trans Biomed Eng*, vol. 69, no. 2, pp. 580–589, Feb. 2022, doi: 10.1109/TBME.2021.3102009.
- [29] D. G. Lloyd and T. F. Besier, "An EMG-driven musculoskeletal model to estimate muscle forces and knee joint moments in vivo," *J Biomech*, vol. 36, no. 6, pp. 765–776, Jun. 2003, doi: 10.1016/s0021-9290(03)00010-1.
- [30] Reed, D. Gurchiek, et al. "Wearable sensors for remote patient monitoring in orthopedics." *Minerva* 72.5 (2021): 484-97.
- [31] McGinnis, Ryan S., et al. "Skin mounted accelerometer system for measuring knee range of motion." 2016 38th Annual International Conference of the IEEE Engineering in Medicine and Biology Society (EMBC). IEEE, 2016.

- [32] Jortberg, Elise, et al. "A novel adhesive biosensor system for detecting respiration, cardiac, and limb movement signals during sleep: Validation with polysomnography." *Nature and science of sleep* 10 (2018): 397.
- [33] P. DasMahapatra, E. Chiauzzi, R. Bhalerao, and J. Rhodes, "Free-Living Physical Activity Monitoring in Adult US Patients with Multiple Sclerosis Using a Consumer Wearable Device," *Digit Biomark*, vol. 2, no. 1, pp. 47–63, 2018, doi: 10.1159/000488040.
- [34] J. E. Thorp, P. G. Adamczyk, H.-L. Ploeg, and K. A. Pickett, "Monitoring Motor Symptoms During Activities of Daily Living in Individuals With Parkinson's Disease," *Front Neurol*, vol. 9, p. 1036, 2018, doi: 10.3389/fneur.2018.01036.
- [35] P. Conway et al., "Rural Health Networks and Care Coordination: Health Care Innovation in Frontier Communities to Improve Patient Outcomes and Reduce Health Care Costs," *J Health Care Poor Underserved*, vol. 27, no. 4A, pp. 91–115, 2016, doi: 10.1353/hpu.2016.0181.
- [36] J. Runkle, M. Sugg, D. Boase, S. L. Galvin, and C. C. Coulson, "Use of wearable sensors for pregnancy health and environmental monitoring: Descriptive findings from the perspective of patients and providers," *DIGITAL HEALTH*, vol. 5, p. 2055207619828220, Jan. 2019, doi: 10.1177/2055207619828220.
- [37] R. D. Gurchiek, N. Cheney, and R. S. McGinnis, "Estimating Biomechanical Time-Series with Wearable Sensors: A Systematic Review of Machine Learning Techniques," *Sensors (Basel)*, vol. 19, no. 23, p. 5227, Nov. 2019, doi: 10.3390/s19235227.
- [38] Gurchiek, Reed D., Anna T. Ursiny, and Ryan S. McGinnis. "A gaussian process model of muscle synergy functions for estimating unmeasured muscle excitations using a measured subset." *IEEE Transactions on Neural Systems and Rehabilitation Engineering* 28.11 (2020): 2478-2487.
- [39] Gurchiek, Reed D., Anna T. Ursiny, and Ryan S. McGinnis. "Modeling muscle synergies as a Gaussian process: Estimating unmeasured muscle excitations using a measured subset." 2020 42nd Annual International Conference of the IEEE Engineering in Medicine & Biology Society (EMBC). IEEE, 2020.
- [40] Gurchiek, Reed D., Anna T. Ursiny, and Ryan S. McGinnis. "Estimating muscle excitations using a reduced sEMG array across a range of walking speeds." *Dynamic Walking*, May (2020).
- [41] D. R. Bell et al., "Objectively Measured Physical Activity in Patients After Anterior Cruciate Ligament Reconstruction," *Am J Sports Med*, vol. 45, no. 8, pp. 1893–1900, Jul. 2017, doi: 10.1177/0363546517698940.

- [42] M. J. Decker, M. R. Torry, T. J. Noonan, W. I. Sterett, and J. R. Steadman, "Gait retraining after anterior cruciate ligament reconstruction 1," *Archives of Physical Medicine and Rehabilitation*, vol. 85, no. 5, pp. 848–856, May 2004, doi: 10.1016/j.apmr.2003.07.014.
- [43] J. Crow, A. Semciw, J. Couch, and T. Pizzari, "Does a recent hamstring muscle injury affect the timing of muscle activation during high speed overground running in professional Australian Football players?," *Phys Ther Sport*, vol. 43, pp. 188–194, May 2020, doi: 10.1016/j.ptsp.2020.03.005.
- [44] A. M. Pearson, "Muscle growth and exercise," *Critical Reviews in Food Science and Nutrition*, vol. 29, no. 3, pp. 167–196, Jan. 1990, doi: 10.1080/10408399009527522.
- [45] C. Bosco et al., "A dynamometer for evaluation of dynamic muscle work," *Eur J Appl Physiol Occup Physiol*, vol. 70, no. 5, pp. 379–386, 1995, doi: 10.1007/BF00618487.
- [46] Moon, Yaejin, et al. "Monitoring gait in multiple sclerosis with novel wearable motion sensors." *PloS one* 12.2 (2017): e0171346.
- [47] Weed, Lara, et al. "A preliminary investigation of the effects of obstacle negotiation and turning on gait variability in adults with multiple sclerosis." *Sensors* 21.17 (2021): 5806.
- [48] C. A. McGibbon, "Toward a Better Understanding of Gait Changes With Age and Disablement: Neuromuscular Adaptation," *Exercise and Sport Sciences Reviews*, vol. 31, no. 2, pp. 102–108, Apr. 2003.
- [49] A. Del Vecchio, A. Úbeda, M. Sartori, J. M. Azorín, F. Felici, and D. Farina, "Central nervous system modulates the neuromechanical delay in a broad range for the control of muscle force," *Journal of Applied Physiology*, vol. 125, no. 5, pp. 1404–1410, Nov. 2018, doi: 10.1152/jappphysiol.00135.2018.
- [50] T. S. Buchanan, D. G. Lloyd, K. Manal, and T. F. Besier, "Neuromusculoskeletal Modeling: Estimation of Muscle Forces and Joint Moments and Movements From Measurements of Neural Command," *J Appl Biomech*, vol. 20, no. 4, pp. 367–395, Nov. 2004.
- [51] J. Cuadrado, F. Michaud, U. Lúgrís, and M. Pérez Soto, "Using Accelerometer Data to Tune the Parameters of an Extended Kalman Filter for Optical Motion Capture: Preliminary Application to Gait Analysis," *Sensors (Basel)*, vol. 21, no. 2, p. 427, Jan. 2021, doi: 10.3390/s21020427.

- [52] S. L. Delp et al., “OpenSim: Open-Source Software to Create and Analyze Dynamic Simulations of Movement,” *IEEE Transactions on Biomedical Engineering*, vol. 54, no. 11, pp. 1940–1950, Nov. 2007, doi: 10.1109/TBME.2007.901024.
- [53] V. Sonone, “Approximating a time series — time series and it’s analysis.,” *Medium*, Oct. 26, 2020. <https://medium.datadriveninvestor.com/approximating-a-time-series-time-series-and-its-analysis-923aa81ca80a> (accessed Nov. 29, 2022).
- [54] C. E. Rasmussen and C. K. I. Williams, *Gaussian processes for machine learning*. Cambridge, Mass: MIT Press, 2006.
- [55] N. A. Bianco, C. Patten, and B. J. Fregly, “Can Measured Synergy Excitations Accurately Construct Unmeasured Muscle Excitations?,” *J Biomech Eng*, vol. 140, no. 1, Jan. 2018, doi: 10.1115/1.4038199.
- [56] Aminian, Kamiar, et al. "Spatio-temporal parameters of gait measured by an ambulatory system using miniature gyroscopes." *Journal of biomechanics* 35.5 (2002): 689-699.
- [57] H. J. Hermens, B. Freriks, C. Disselhorst-Klug, and G. Rau, “Development of recommendations for SEMG sensors and sensor placement procedures,” *J Electromyogr Kinesiol*, vol. 10, no. 5, pp. 361–374, Oct. 2000, doi: 10.1016/s1050-6411(00)00027-4.
- [58] B. Mijovic, M. B. Popovic, and D. B. Popovic, “Synergistic control of forearm based on accelerometer data and artificial neural networks,” *Braz J Med Biol Res*, vol. 41, no. 5, pp. 389–397, May 2008, doi: 10.1590/s0100-879x2008005000019.
- [59] A. Findlow, J. Y. Goulermas, C. Nester, D. Howard, and L. P. J. Kenney, “Predicting lower limb joint kinematics using wearable motion sensors,” *Gait Posture*, vol. 28, no. 1, pp. 120–126, Jul. 2008, doi: 10.1016/j.gaitpost.2007.11.001.
- [60] M. Grimmer, K. Schmidt, J. E. Duarte, L. Neuner, G. Koginov, and R. Riener, “Stance and Swing Detection Based on the Angular Velocity of Lower Limb Segments During Walking,” *Frontiers in Neurorobotics*, vol. 13, 2019, Accessed: Dec. 01, 2022. [Online]. Available: <https://www.frontiersin.org/articles/10.3389/fnbot.2019.00057>
- [61] A. Nandy, S. Chakraborty, J. Chakraborty, and G. Venture, “1 - Introduction,” in *Modern Methods for Affordable Clinical Gait Analysis*, A. Nandy, S. Chakraborty, J. Chakraborty, and G. Venture, Eds. Academic Press, 2021, pp. 1–15. doi: 10.1016/B978-0-323-85245-6.00012-6.
- [62] N. A. Turpin, S. Uriac, and G. Dalleau, “How to improve the muscle synergy analysis methodology?,” *Eur J Appl Physiol*, vol. 121, no. 4, pp. 1009–1025, Apr. 2021, doi: 10.1007/s00421-021-04604-9.

- [63] M. J. Escalona, D. Bourbonnais, M. Goyette, D. Le Flem, C. Duclos, and D. H. Gagnon, “Effects of Varying Overground Walking Speeds on Lower-Extremity Muscle Synergies in Healthy Individuals,” *Motor Control*, vol. 25, no. 2, pp. 234–251, Jan. 2021, doi: 10.1123/mc.2020-0008.
- [64] “Gait Cycle - an overview | ScienceDirect Topics.” <https://www.sciencedirect.com/topics/engineering/gait-cycle> (accessed Dec. 01, 2022).
- [65] L. Kohn, E. Rembeck, and A. Rauch, “[Anterior cruciate ligament injury in adults : Diagnostics and treatment],” *Orthopade*, vol. 49, no. 11, pp. 1013–1028, Nov. 2020, doi: 10.1007/s00132-020-03997-3.
- [66] J. Evans and J. I Nielson, “Anterior Cruciate Ligament Knee Injuries,” in *StatPearls*, Treasure Island (FL): StatPearls Publishing, 2022. Accessed: Nov. 29, 2022. [Online]. Available: <http://www.ncbi.nlm.nih.gov/books/NBK499848/>
- [67] J. M. Losciale, R. M. Zdeb, L. Ledbetter, M. P. Reiman, and T. C. Sell, “The Association Between Passing Return-to-Sport Criteria and Second Anterior Cruciate Ligament Injury Risk: A Systematic Review With Meta-analysis,” *J Orthop Sports Phys Ther*, vol. 49, no. 2, pp. 43–54, Feb. 2019, doi: 10.2519/jospt.2019.8190.
- [68] A. Carbone and S. Rodeo, “Review of current understanding of post-traumatic osteoarthritis resulting from sports injuries,” *J Orthop Res*, vol. 35, no. 3, pp. 397–405, Mar. 2017, doi: 10.1002/jor.23341.
- [69] T. P. Andriacchi and A. Mündermann, “The role of ambulatory mechanics in the initiation and progression of knee osteoarthritis,” *Curr Opin Rheumatol*, vol. 18, no. 5, pp. 514–518, Sep. 2006, doi: 10.1097/01.bor.0000240365.16842.4e.

APPENDIX

BF = Biceps Femoris
CNS = Central Nervous System
CP = Cerebral Palsy
EMG = Electromyography
HD = Huntington's Disease
IMU = Inertial Measurement Unit
LG = Lateral Gastrocnemius
MG = Medial Gastrocnemius
MS = Multiple Sclerosis
NMS = Neuromusculoskeletal
PCB = Printed Circuit Board
PD = Parkinson's Disease
PL = Peroneus Longus
PwMS = Persons with Multiple Sclerosis
RF = Rectus Femoris
SOL = Soleus
ST = Semitendinosus
TA = Tibialis Anterior
VM = Vastus Medialis
VL = Vastus Lateralis